SPARC-MM-06/001
10 May 2006

THE SPARC STEERING MAGNETS:

MEASUREMENTS ON THE BEAM POSITION MONITOR STEERING PROTOTYPE

B. Bolli, S. Ceravolo, P. Iorio, F. Iungo, C. Ligi, M. Paris,
M. Preger, C. Sanelli, F. Sardone, F. Sgamma, M. Troiani,
G. Bazzano, D. Bianculli*, I. De Cesaris**

INFN-LNF
**Fondazione CNAO*

Abstract

The electrical and magnetic measurements made on the beam position monitors (BPM) steering magnets prototype for SPARC, in comparison with the results of the 3D simulations, are reported.

1. Introduction

7 couples of horizontal plus vertical steering magnets have been designed to be placed around 7 BPMs of the SPARC linac. These air-dominated magnets, as the SPARC Section steering magnets [1], have *cos(θ)*–like coils, with the copper conductor wound on an aluminum support. Each couple of magnets consists of an internal magnet surrounded by an external one generating a magnetic field perpendicular to the first one. The internal magnet is mechanically fixed to the external one, and all the structure is maintained in position by an aluminum support (see Figure 1). The magnet design, and especially the coil ends shape, has been chosen due to the reduced longitudinal space near the BPMs. In this way it is possible to correct the beam position both in the horizontal and vertical planes at the same place.

In this prototype the internal magnet has been positioned as an horizontal steering (vertical magnetic field) and the external one as a vertical steering (horizontal magnetic field), but in principle the magnet mechanical support allows the rotation of the magnets by 90 degrees. Table I lists the main parameters required for these magnets, while Table II shows a comparison between the calculated and the measured value of some main magnetic parameters. The magnetic simulations were made by means of the 3D code OPERA, rel. 10.5.

Table I – *BPM Steering Magnets design parameters*

	Units	**Value (Horiz.)**	**Value (Vert.)**
Energy (max)	MeV	230	230
Deflection angle (max)	mrad (@ 230 MeV)	0.51	0.51
Copper Wire Diameter	mm	3	3
Magnet Radius	mm	49	84
Maximum Current	A	15	30

Table II – *BPM Steering Magnets calculation and measurements results*

	Units	**Value (Horiz.)**		**Value (Vert.)**	
		Calc.	*Meas.*	*Calc.*	*Meas.*
Field @ Max. Current	Gauss	36.2	41.1	29.0	32.3
Field Homogeneity @ ±10mm	*ΔB/B*	$3.4*10^{-3}$	$2.7*10^{-3}$	$2.0*10^{-3}$	$3.0*10^{-3}$
Magnetic Length	mm	117	122	138	136

Figure 1: The BPM steering magnet prototype

2. Electrical Measurements

Magnet resistances were measured by means of the Volt-Ampere method at room temperature using the following instrumentation:

Power supply: FUG NLB 700-20
Voltmeter: Fluke mod. 77

The following values were measured at T_{amb} = 23 °C:

Horizontal Steering: $\Delta V = 0.810$ V @ $I = 15$ A $\Leftrightarrow$ $R = 0.054\ \Omega$
Vertical Steering: $\Delta V = 1.914$ V @ $I = 30$ A $\Leftrightarrow$ $R = 0.064\ \Omega$

The inductance and resistance of the steering magnets were also measured by means of a LCR meter, HP mod. 4284 A, at different frequencies. Results are shown in Figure 2. Table III lists the measured values, which are consistent with the design data.

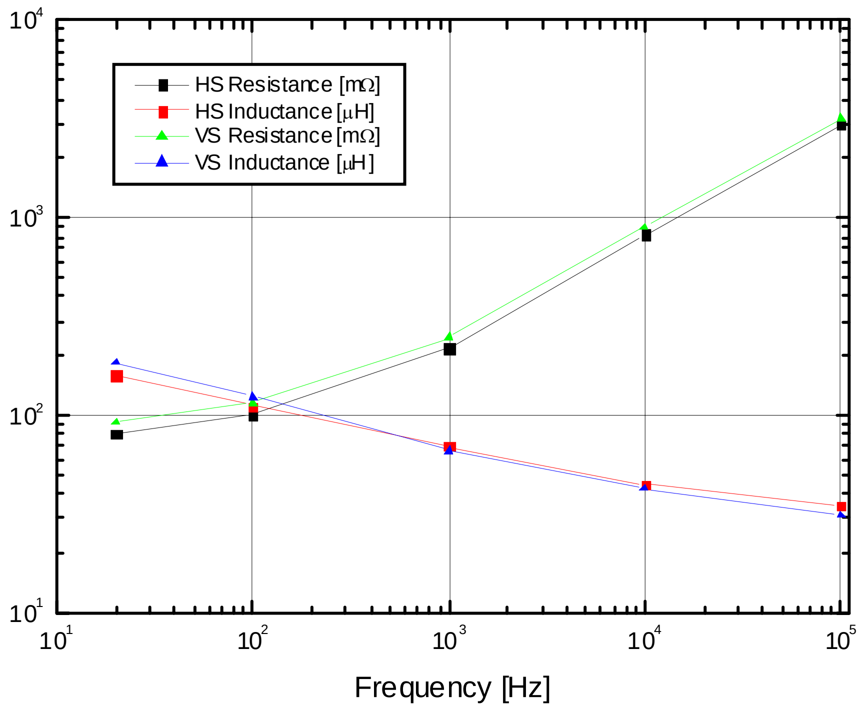

Figure 2: Steering magnet Resistance and Inductance versus frequency

Table III – *Resistance and Inductance versus frequency.*

	Horiz. Steering (internal magnet)		**Vert. Steering (external magnet)**	
Frequency (Hz)	***R* (mΩ)**	***L* (μH)**	***R* (mΩ)**	***L* (μH)**
20	81.0	161	91.6	184
100	101	112	116	125
1 k	219	70.2	247	66.1
10 k	828	44.6	896	42.3
100 k	3005	34.6	3224	31.3

Figure 3 shows the temperature increase on the coil of the two magnets and the aluminum support of one magnet when both magnets are powered at the maximum current. The experimental data have been fitted with the exponential function indicated in the graph.

The room temperature was ≈ 22 °C. Measurements are in good agreement with an expectation of $\Delta T \approx 14$ °C for the Horizontal Steering coil and of $\Delta T \approx 34$ °C for the Vertical Steering coil. Note that the typical temperature rise time is of the order of $3\tau \approx 1.5$ hours.

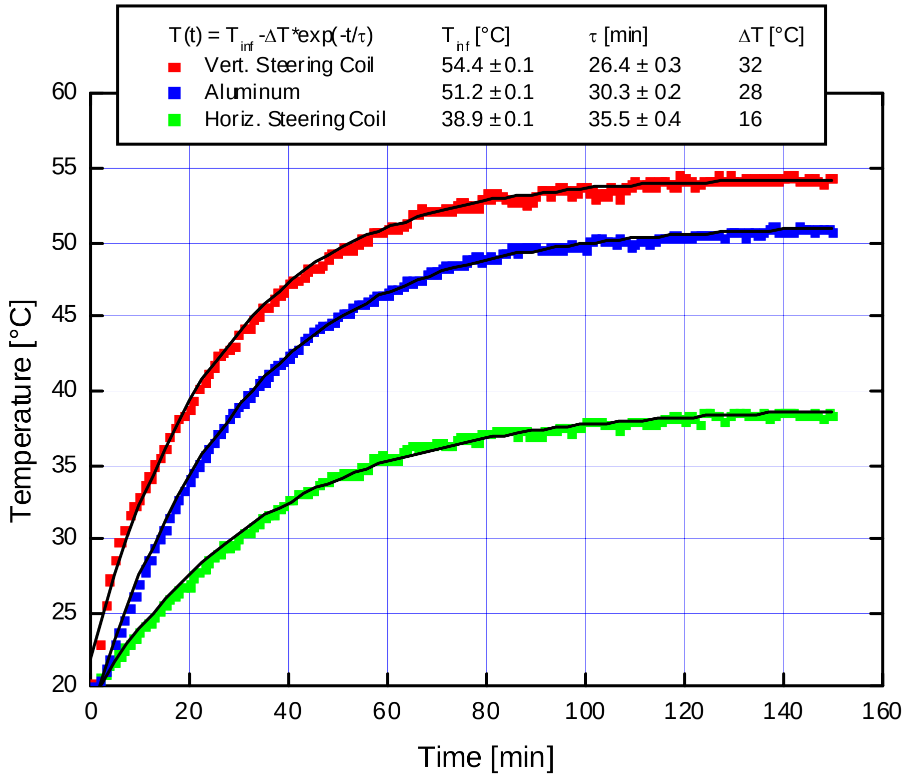

Figure 3: Temperature increase on the coils and the aluminum supports

3. Magnetic Measurements

All the magnetic measurements have been taken with the internal magnet positioned as a horizontal steering, therefore the external magnet acts as a vertical corrector. In the following, x is the transverse horizontal, y the longitudinal (the beam direction) and z the transverse vertical coordinate.

A new Hall probe with a resolution of 10^{-3} Gauss and an accuracy of 0.2 Gauss (0.006% of the full scale) has been used.

The earth magnetic field in the transverse directions has been measured to be

$$B_x = -\,0.360 \text{ Gauss}, \quad B_z = 0.592 \text{ Gauss}$$

This component has not been subtracted from the measured values reported in this paper.

Figure 4 and Figure 5 illustrate two outputs of the TOSCA solver simulations. They show the vectors of the direction of the total field B and the colours of the amplitude of B_z (Figure 4) or B_x (Figure 5) in the vertical plane. Due to the absence of any ferromagnetic material, only the magnet coils have been considered in the simulations.

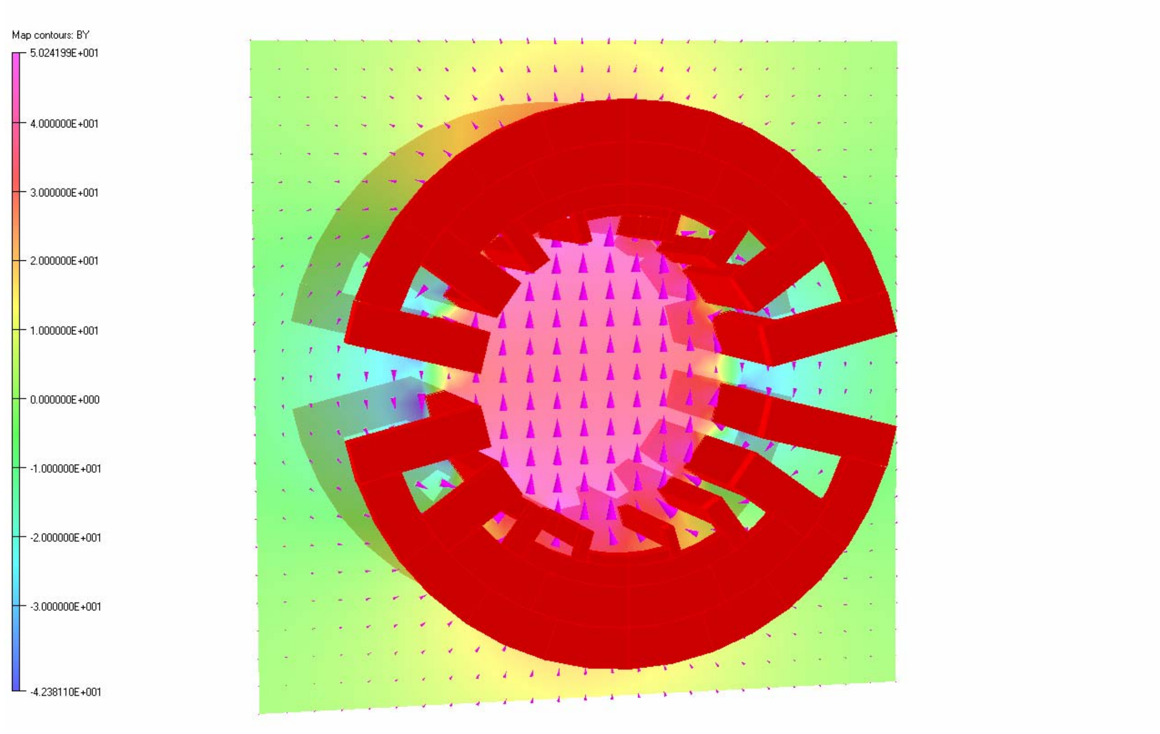

Figure 4: OPERA-3D simulation of the magnetic field in the vertical plane at magnet centre of the Horizontal Steering (internal magnet)

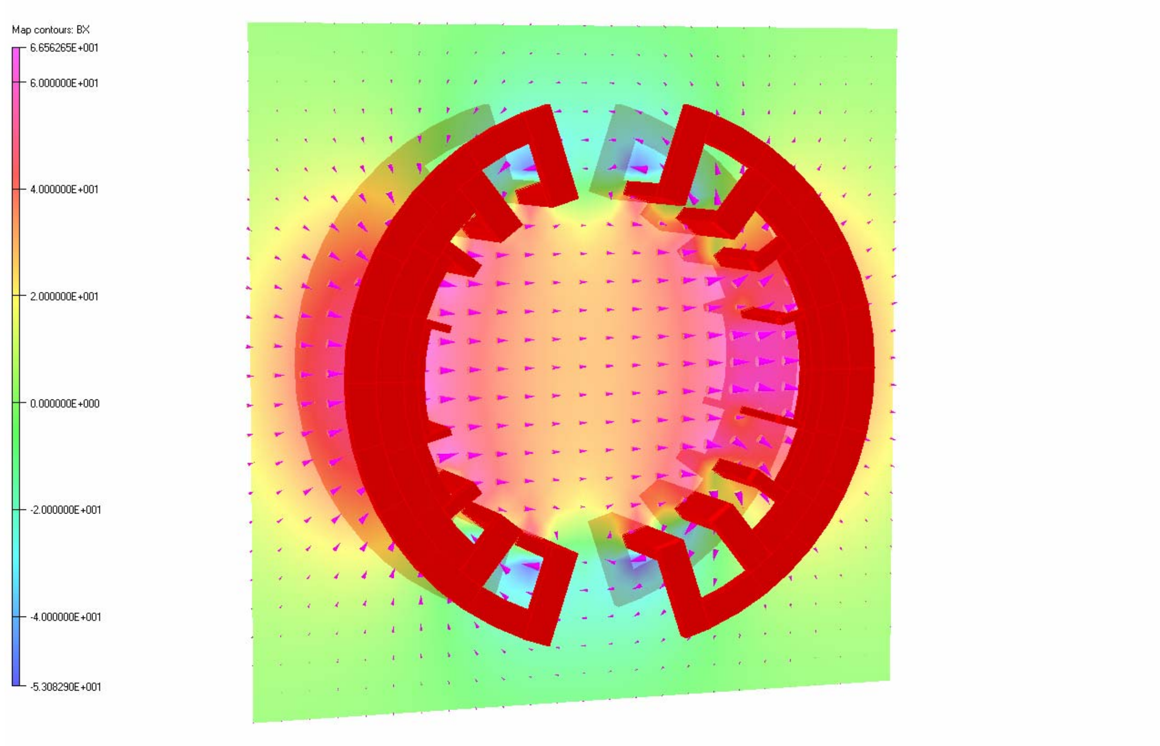

Figure 5: OPERA-3D simulation of the magnetic field in the vertical plane at magnet centre of the Vertical Steering (external magnet)

Figure 6 shows the measured fields at the magnet centre as a function of the current on both the magnets. The current values span from 0 A to the nominal value of the current. Since there is no iron, the field-current curve is absolutely linear, and the measurement confirms the design expectations. The earth magnetic field, at zero current, gives a negligible offset.

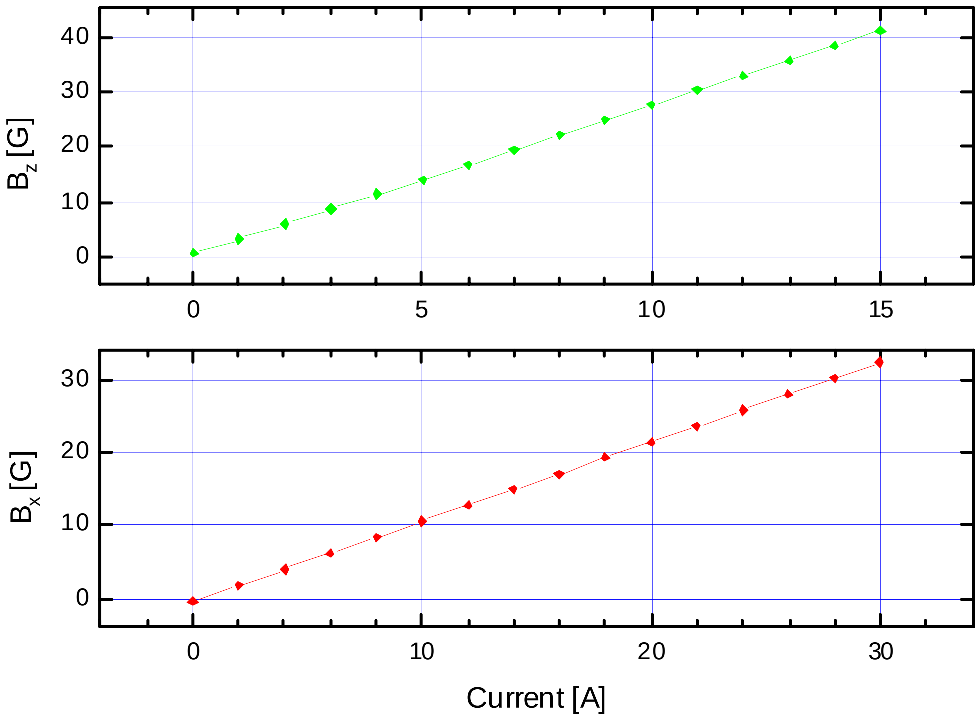

Figure 6:
***up*: B_z at the magnet centre versus current on the Horizontal Steering (internal magnet)**
***down*: B_x at the magnet centre versus current on the Vertical Steering (external magnet)**

The field behaviour has been measured in steps of 10 mm along the longitudinal axis *y*, in steps of 5 mm in one of the transverse axis (*x* in the horizontal steering and *z* in the vertical steering) and in steps of 7 mm in the other transverse axis. We remind that the requested good field is within ± 10 mm (see Table I), but the measurements have been extended till ± 15 mm.

The measured field values are in quite good agreement with those obtained simulating the magnets by means of the 3D code OPERA. Figure 7 shows the measured and calculated main component of the field versus the transverse position (horizontal on the first and vertical on the second plot) at magnet centre ($y = 0$) and at the maximum current value. The measured value, when subtracted the earth magnetic field, is 12% higher than the expected in the horizontal steering and 13% higher in the vertical one. Those differences are probably due to the approximation made in the coil end shape definition in the simulations. Nevertheless the measured field quality inside the good field region (±10 mm) is $\Delta B/B$ = 2.7 10^{-3} in the horizontal steering and $\Delta B/B$ = 3.0 10^{-3} in the vertical one, in good agreement with the calculated values (see Table II).

Figure 8 shows the measured main component of the field in the transverse position, as the previous plots, at different *z* (first plot) and *x* (second plot) positions. There is a small right-left asymmetry in the measured data, but only far from the central axis. As we will see later, the differences between the values of the three curves on the plots do not affect the uniformity of the integrated fields on the longitudinal position.

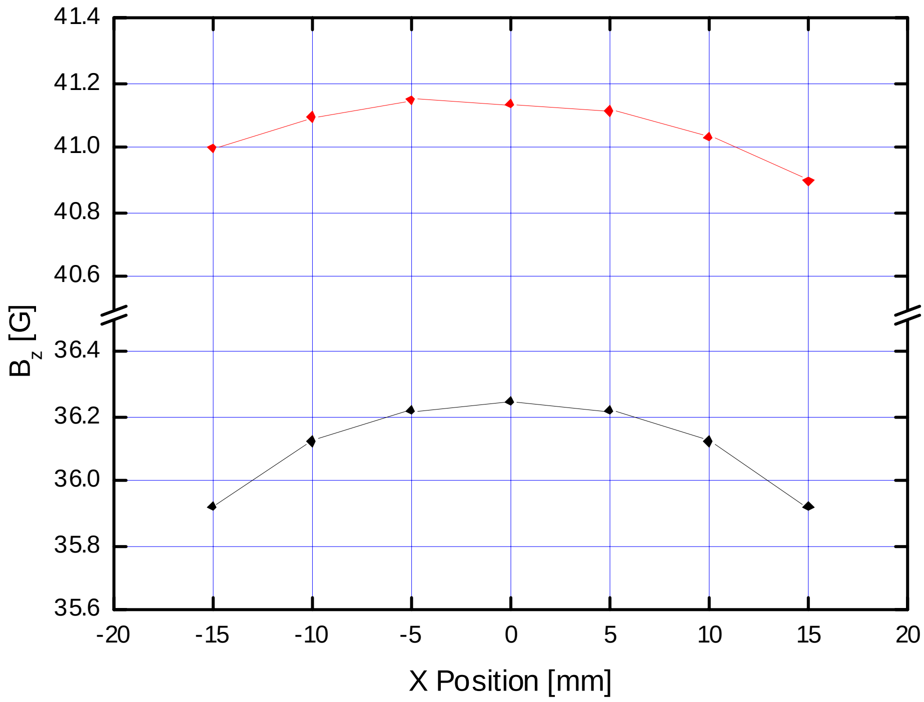

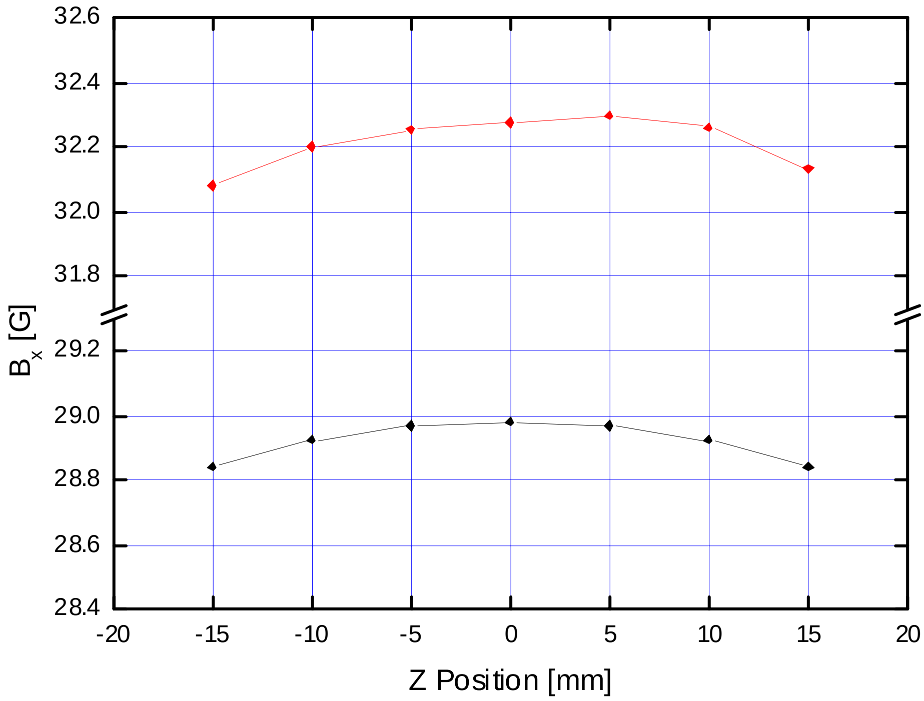

Figure 7:
***up*: measured (red) and calculated (black) B_z at the magnet center versus the horizontal position @ 15 A on the Horizontal Steering (internal magnet)**
***down*: measured (red) and calculated (black) B_x at the magnet center versus the vertical position @ 30 A on the Vertical Steering (external magnet)**

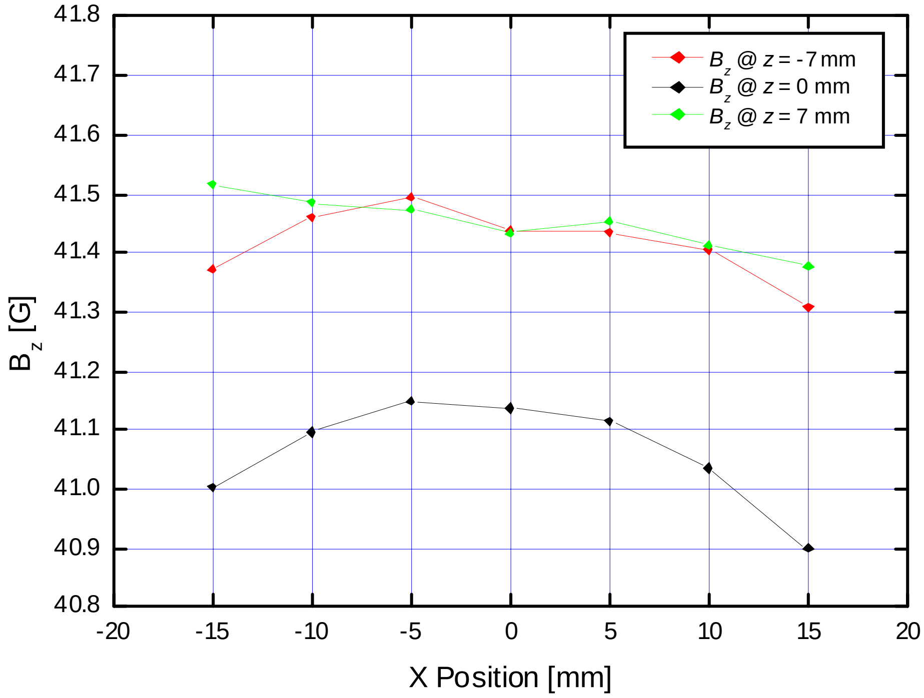

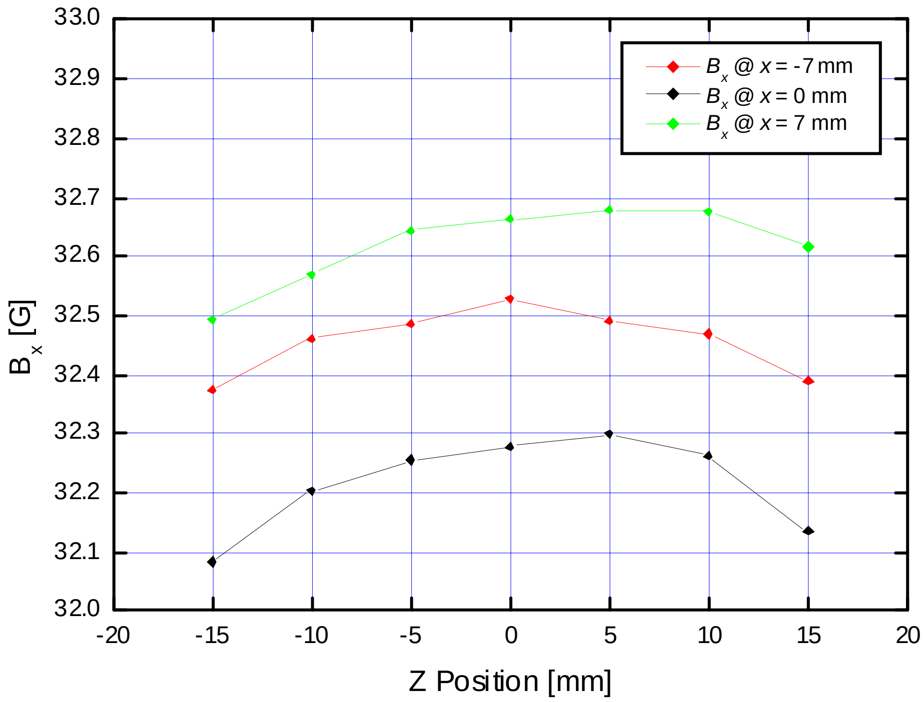

Figure 8:
up: **Measured B_z at y = 0 versus the vertical position @ 15 A for different vertical positions on the Horizontal Steering (internal magnet)**
down: **Measured B_x at y = 0 versus the horizontal position @ 30 A for different vertical positions on the Vertical Steering (external magnet)**

Figure 9 shows the comparison between the measured and calculated main component of the field along the magnet axis in the two magnets. The full width at half maximum is 110.3 mm on the horizontal steering and 129.2 mm on the vertical one. From the figures a small shift of ≈ – 0.3 mm between the two curves on both the magnets has been noticed.

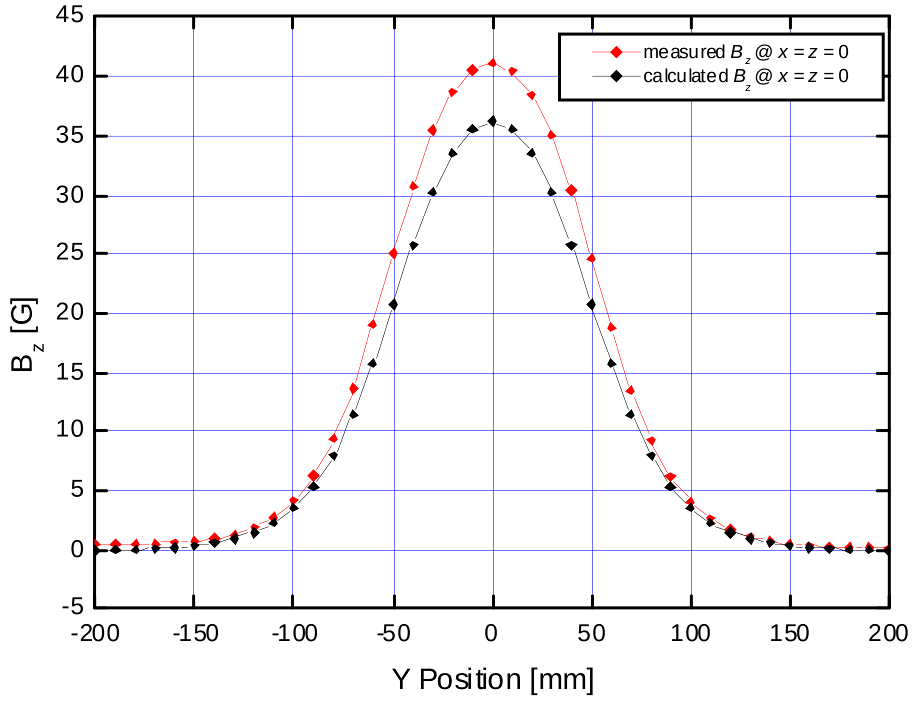

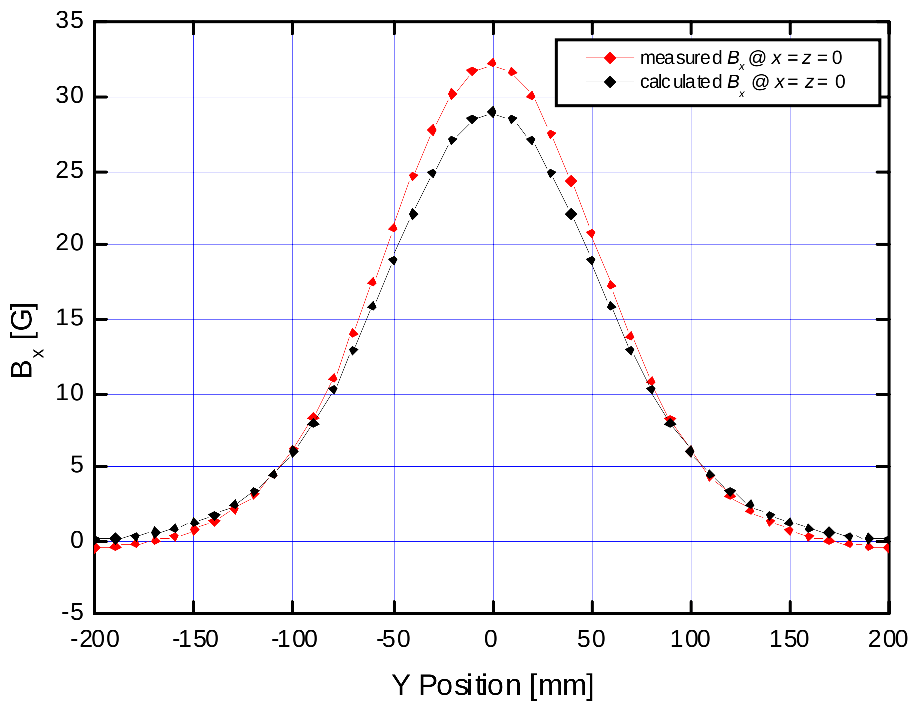

Figure 9:

***up*: measured (red) and calculated (black) B_z at the magnet center versus the longitudinal position @ 15 A on the Horizontal Steering (internal magnet)**

***down*: measured (red) and calculated (black) B_x at the magnet center versus the longitudinal position @ 30 A on the Vertical Steering (external magnet)**

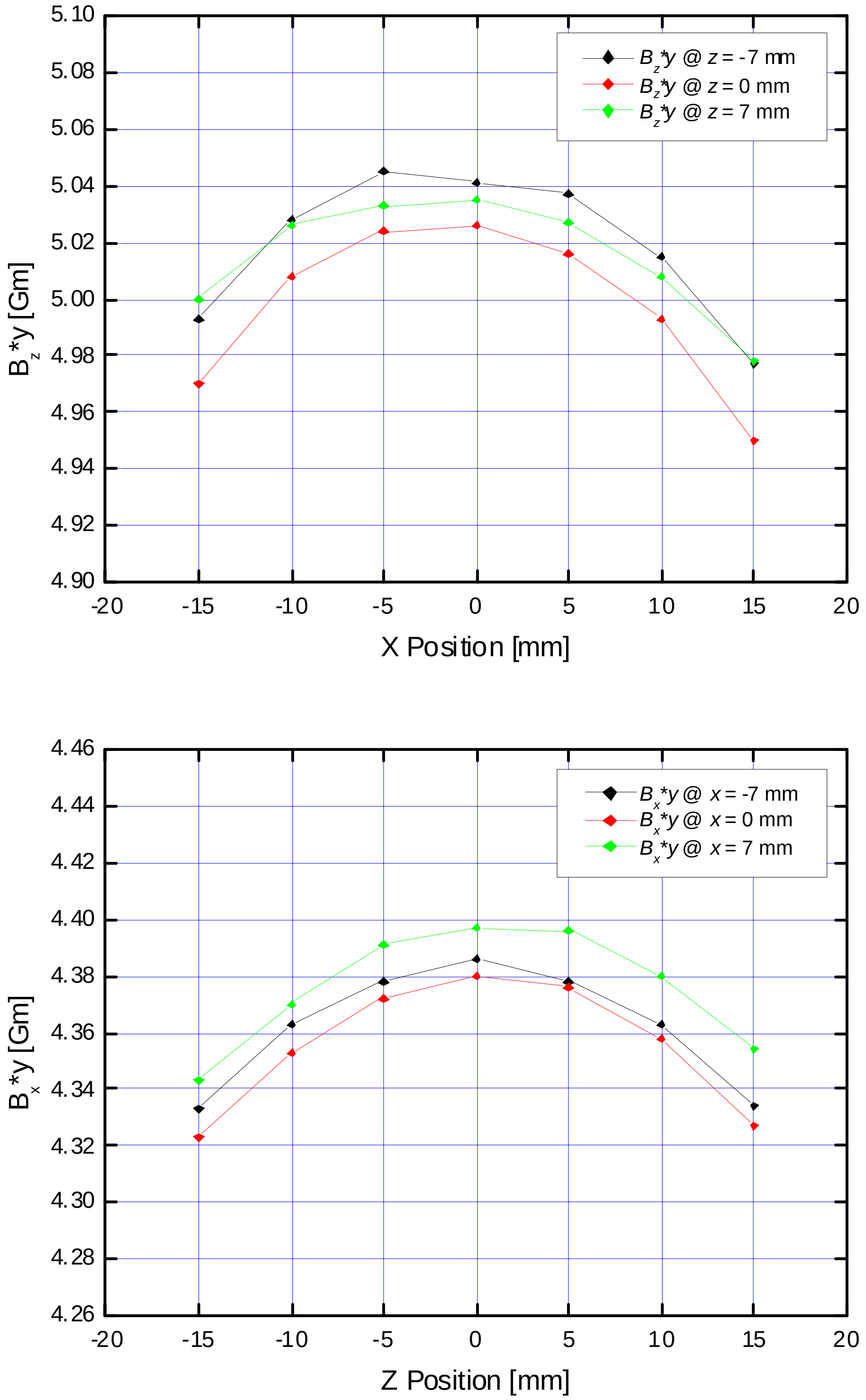

Figure 10:
up: **integrated vertical component of the field versus the horizontal position @ 15 A for different vertical positions, on the Horizontal Steering (internal magnet)**
down: **integrated horizontal component of the field versus the vertical position @ 30 A for different horizontal positions, on the Vertical Steering (external magnet)**

The integrated main component of the magnetic field along the longitudinal position between ±200 mm from the centre is given in Figure 10 for the two magnets as function of the x (first plot) and z (second plot) coordinate, respectively. It must be noticed that the integrated field on both the magnets never differs from the center value ($x = z = 0$) by more than ± 0.7% in the good field region.

The measured magnetic length is 122 mm for the internal magnet and 136 mm for the external one, in good agreement with the expectations (see Table II).

Thanks to the linearity of the field versus current (Figure 6), taking the average value of the integrated field measured in the good field region, the angular kick α on the two magnets can be expressed as a function of the beam energy and the excitation current as:

$$\alpha\,(\text{mrad}) = 10.1 * 10^{-3} * \text{I (A)} / \text{E (GeV)} \quad \text{(internal magnet)}$$
$$\alpha\,(\text{mrad}) = 4.38 * 10^{-3} * \text{I (A)} / \text{E (GeV)} \quad \text{(external magnet)}$$

4. Conclusions

The SPARC BPM steering magnet prototype has been fully characterised, and the measurements confirmed the reliability of its magnetic design. The quality of the field is in good agreement with the simulations, the peak and integrated values being slightly larger than expected. The integrated magnetic field on the longitudinal direction is quite constant in the good field region.

The compactness of the design allows the insertion of the two correctors in a very small longitudinal zone, such as around the SPARC beam position monitors. The linearity of the magnetic field with the excitation current makes the overall orbit correction procedure easier.

References

[1] B. Bolli et al.: *The SPARC Steering Magnets: Measurements on the Accelerating Section Steering Prototype*, SPARC Technical Note MM-05/002 (2005)